

Research Article

Bone marrow-derived cells or C-X-C motif chemokine 12 (CXCL12) treatment improve thin endometrium in a mouse model[†]

Kyong Wook Yi^{1,2}, Ramanaiah Mamillapalli^{1,*}, Cagdas Sahin¹,
Jaeyen Song¹, Reshef Tal¹ and Hugh S. Taylor¹

¹Department of Obstetrics and Gynecology, Reproductive Sciences, Yale School of Medicine, New Haven, Connecticut, USA and ²Department of Obstetrics and Gynecology, Korea University College of Medicine, Seoul, Republic of Korea

***Correspondence:** Department of Obstetrics, Gynecology and Reproductive Sciences, Yale School of Medicine, 310 Cedar Street, New Haven, CT 06510, USA. Tel: +203-737-8082; Fax: +203-785-4713; E-mail: ramana.mamillapalli@yale.edu

[†]**Grant Support:** This work was supported by the National Institutes of Health NIH R01 HD052668 to HST

Conference Presentation: Presented in part at the 65th Annual Meeting of the Society for Reproductive Investigation (SRI), 6–10 March 2018, San Diego, CA, USA (Abstract O-121).

Edited by Dr. Haibin Wang, PhD, Xiamen University

Received 12 February 2018; Revised 14 July 2018; Accepted 30 July 2018

Abstract

Successful implantation and pregnancy is dependent on sufficient endometrial growth during each reproductive cycle. Here, we report the therapeutic effect of either bone marrow-derived cells (BMDCs) or the stem cell chemo-attractant C-X-C motif chemokine 12 (CXCL12) on endometrial receptivity in a murine ethanol induced thin endometrium model. Endometrial epithelial area was significantly increased in mice treated with BMDCs, CXCL12, or by co-treatment with both compared with PBS-treated controls. Ki-67 and CD31 immunoreactivity was significantly higher in mice treated with either BMDCs, CXCL12, or both. The mRNA expression levels of endometrial receptivity markers leukemia inhibitory factor, interleukin-1 β , and integrin beta-3 were increased in mice treated with either BMDCs, CXCL12, or both. The mRNA levels of matrix metalloproteinase-2 and -9 were significantly decreased by BMDCs but not by CXCL12. Pregnancy rates and litter size were increased after either treatment. Both BMDCs and CXCL12 displayed a comparable efficacy on endometrial regeneration in mice with thin endometrium. Our findings indicate the potential therapeutic effects of BMDCs and CXCL12 on infertility related to thin endometrium. Bone marrow-derived cells and CXCL12 displayed a comparable efficacy on endometrial regeneration in mice with thin endometrium.

Summary Sentence

Bone marrow-derived cells and CXCL12 displayed a comparable efficacy on endometrial regeneration in mice with thin endometrium.

Key words: bone marrow-derived cells (BMDCs), CXCL12, thin endometrium, infertility.

Introduction

Adequate endometrial growth during the reproductive cycle is an essential factor to achieve successful implantation and pregnancy. This physiology is further regulated by various complex molecules

such as endogenous sex steroid hormones, growth factors, and cytokines. Human endometrial development is frequently monitored using transvaginal ultrasound in assisted reproductive technology (ART) cycles. Endometrial thickness is a well-established marker

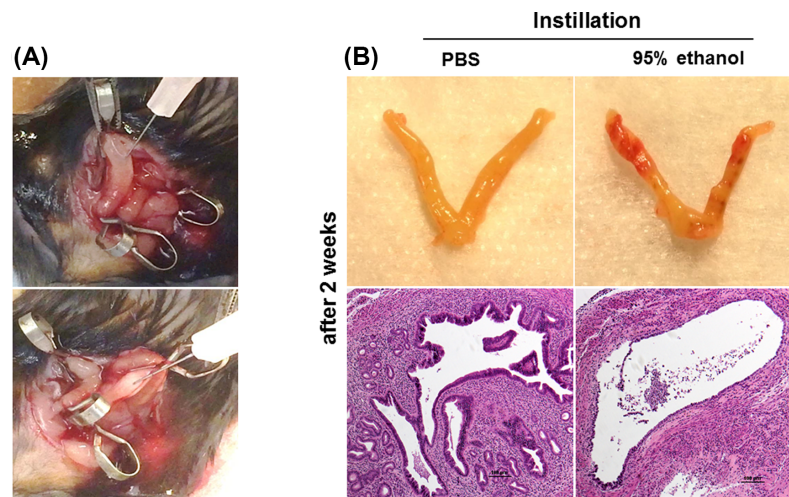


Figure 1. (A) Images from treatment modeling of thin EM. (B) Gross and micrograph images (H&E $\times 100$) of the uterine horns 2 weeks after injection of PBS (left) or 95% ethanol (right) into the uterine cavity from pilot experiments.

of uterine receptivity. Although there is no standardized value of endometrial thickness for diagnosis of a thin endometrium (EM), 7 mm has been suggested as the minimal cutoff for embryo transfer, with an endometrial thickness greater than 9 mm predicting higher implantation rates and more favorable outcomes [1–3]. Indeed, many have consistently reported that persistently thin EM during a monitored reproductive cycle is associated with lower implantation rates or increased miscarriage rates [4–6]. Therefore, many have sought to identify the therapeutic modalities that could improve endometrial growth and receptivity in women with a thin EM. Several clinical treatment approaches, including low-dose aspirin, sildenafil, or granulocyte colony-stimulating factor have been tried; however, the results have been inconclusive [7–10].

Recent evidence has implicated bone marrow-derived stem cells (BMDSCs) in the physiological regeneration of the EM in each reproductive cycle, and has further highlighted the potential roles of BMDSCs in repairing a spectrum of endometrial pathologies [11–13]. Our previous studies demonstrated that BMDSCs contribute to endometrial regeneration and repair in response to mechanical or ischemic reperfusion injuries to the uterine EM in murine models [11, 14, 15].

C-X-C motif chemokine 12 (CXCL12, also known as stromal-derived factor-1) is a potent chemotactic factor that is predominantly produced by BM stromal cells and endothelial cells across many organs [16, 17]. CXCL12 functions in the modulation of the immune system via lymphocyte migration, development, or survival [18–20], and mediates the mobilization and homing of BM stem/progenitor cells to injured microenvironments [20, 21]. We previously described that the *in vitro* treatment of human endometrial stromal cells with CXCL12 significantly enhances the migration of BMDSCs towards uterine stromal cells [22]. In addition, the augmentation of CXCL12 following uterine injury increased BMDSC engraftment to the uterus in a mouse model [13].

Considering the biological properties of CXCL12 related to the modulation of the immune system and stem cell biology, we hypothesized that CXCL12 plays a beneficial role for endometrial regeneration in impaired endometrial growth and in the improvement of endometrial receptivity related to thin EM. This study aimed to determine the therapeutic effects of both CXCL12 and bone marrow-derived cells (BMDCs) individually or in combination in a murine model, following induction of thin EM.

Materials and methods

Animals

C57 BL/6 female mice and ubiquitin-green fluorescent protein (GFP) male mice were purchased from the Charles River Laboratories (Wilmington, MA) and Jackson Laboratory (Bar Harbor, ME), respectively. All mice were housed with free access to food and water, and were maintained in a room ($21 \pm 1^\circ\text{C}$) with a regular 12 h light/dark cycle (7:00 a.m. to 7:00 p.m.) in the Yale Animal Resources Center (YARC) at Yale University School of Medicine. All animal experiments were carried out with the protocol approved by the YARC and approved by the Institutional Animal Care and Use Committee at Yale University.

Induction of thin EM and treatment with BMDCs and CXCL12

Thin EM was induced in female mice (8 to 10 weeks old) using 95% ethanol as described previously [23–25]. The mice were anesthetized by isoflurane inhalation and the uterus was gently exposed through an abdominal incision. Atraumatic vascular clips were applied at the proximal and distal ends of the bilateral uterine horns and then 50 μL of 95% anhydrous ethanol or phosphate-buffered saline (PBS) as a control was instilled into the uterine cavity using a 1 mL tuberculin syringe equipped with a 30G needle (Figure 1A). Five minutes later, the clips were removed and the uterine cavity was flushed with sterile PBS to eliminate any remaining ethanol.

To determine the effects of agents that were designed to improve endometrial regeneration, five treatment groups were generated. One group received sham surgery without ethanol administration as a control for the effects of the procedure. Mice with ethanol-induced thin EM were randomly divided into four treatment groups ($n = 5$ for each group): (i) PBS (200 μL /mouse, local injection), (ii) recombinant CXCL12 (Sigma-Aldrich, St. Louis, MO, USA; 2 μg /mouse, local injection), (iii) systemic administration of BMDCs, and (iv) co-treatment with CXCL12 and BMDCs. CXCL12 or PBS was administered through local injection to the uterine muscle layer in at least three different sites. BMDCs were harvested from 6 to 8-week-old GFP male mice by flushing the marrow cavity of the femur and tibia with cold sterile Dulbecco modified Eagle medium F-12, (Thermo

Fisher Scientific, Waltham, MA) and filtering through a sterile 70 μm nylon mesh (Thermo Fisher Scientific). The yield and viability of BMDCs were determined by Trypan blue staining. BMDCs in 100 μL PBS (30×10^6 cells/mouse) were administered through a retro-orbital injection 4 to 6 h following the surgery.

Three to four estrous cycles (14 ± 2 days) after surgery and treatments, the mice were sacrificed at their estrous phase, and the uterine tissues were obtained. In order to examine the functional improvement in fertility, female mice from all experimental groups ($n = 5$ in each group) were mated with wild-type C57 BL/6 proven male mice after two estrous cycles after modeling and treatment with BMDCs or CXCL12.

RNA extraction and quantitative real-time polymerase chain reaction

Uterine tissue (50–100 mg) was homogenized using 1 mL TRIzol reagent (Life Technologies, Carlsbad, CA), and total RNA was extracted according to the manufacturer's protocol. The total RNA was purified using the RNeasy MinElute Cleanup Kit (Qiagen, Valencia, CA), and RNA concentration was determined by Nanodrop ND-2000 spectrophotometer (Thermo Fisher Scientific). The first strand cDNA was synthesized from purified RNA by reverse transcription using an iScript cDNA synthesis kit (Bio-Rad Laboratories, Hercules, CA) in T100 thermal cycler (Bio-Rad). Quantitative real-time polymerase chain reaction (qRT-PCR) was performed using SYBR Green (Bio-Rad Laboratories) and optimized in the CFX Connect real-time PCR detection system (Bio-Rad Laboratories). The specificity of the amplified transcript and the absence of primer dimers were confirmed by a melting curve analysis. All products yielded the predicted melting temperature. The primer sequences used in this study: leukemia inhibitory factor (LIF): forward, 5'-CCCATCACCCCTGTAAAT-3', and reverse, 5'-GTTAGGCGCACATAGCTT-3'; integrin α -v (ITG α v): forward, 5'-GGCACAAAGACCGTTGAGTA-3', and reverse, 5'-GCCACTTGGTCCGAAATGAG-3'; integrin β -3 (ITG β 3): forward, 5'-TGCTCCAGAGTCTATTGAGTTCC-3', and reverse, 5'-GAGAAAGACAGGTCCATCAAGTAG-3'; interleukin-6 (IL-6): forward, 5'-TAGTCCTTCTACCCCAATTTCC-3', and reverse, 5'-TTGGTCTTAGCCACTCCTTC-3'; interleukin-1 β (IL-1 β): forward, 5'-TGCCACCTTTTGACAGTGATG-3', and reverse, 5'-AAGGTCCACGGGAAAGACAC-3'; matrix metalloproteinase-2 (MMP-2): forward, 5'-CCCTCAAGAAGATGCAGAAGTTC-3', and reverse, 5'-TCTTGCTTCCGCATGGT-3'; matrix metalloproteinase-9 (MMP-9): forward, 5'-CGTCATTCGCGTGGATAAGG-3' and reverse, 5'-TTTGAAACTCACACGCCAG-3'; and β -actin: forward, 5'-AGTGTGACGTTGACATCCGTA-3', and 5'-GCCAGAGCAGTAATCTCCTTCT-3'.

qPCR was carried out for 39 cycles of denaturation at 95°C for 10 s following activation at 95°C for 3 min, and annealing at 60°C for 30 s. The specificity of the amplified transcript and absence of primer-dimers was confirmed by a melting curve analysis. Gene expression was normalized to that of β -actin as an internal control. Relative mRNA expression was calculated using the comparative cycle threshold method ($2^{-\Delta\Delta C_t}$) [26, 27].

Immunohistochemistry and immunofluorescence

Tissue was fixed in 4% paraformaldehyde and embedded in paraffin. Uterine tissue sections were deparaffinized followed by dehydration/hydration with xylene and ethanol. Antigen retrieval was

performed in 0.01 mol/L sodium citrate buffer (pH 6) for 15 min. Endogenous peroxidase activity was blocked using 3% hydrogen peroxide in methanol for 10 min, and then nonspecific binding was blocked with 5% normal goat or rabbit serum. The sections were incubated overnight at 4°C with different primary antibodies anti-Ki-67, (#ab15580, 1:500), anti-CD45 (#ab25286; 1:300); anti-CD31 (#ab28364, 1:200), anti-LIF (#ab138002, 1:200), anti-GFP (#ab6556, 1:1000) purchased from Abcam, Cambridge, MA, USA. The dilution of each primary antibody was made according to the guidelines from the manufacturer. After three washes with PBS, the sections were incubated at room temperature with appropriate biotinylated secondary antibody (1:200; Vector Laboratories) for 1 h, and the signal was detected using ABC Vectastain Elit reagents with DAB plus H₂O₂ (#SK-4105; Vector Laboratories). Tissue sections were counterstained with hematoxylin (Sigma-Aldrich, St. Louis, MO, USA). Images of stained sections were captured using Olympus BX-51 microscope (Olympus). For colocalization of GFP-positive BMDCs by immunofluorescence, sections were incubated with anti-GFP (#ab6556, 1:1000), anti-CD45 (#ab25286; 1:300), and anti-F4/80 (#ab111101, 1:160) antibodies. Secondary antibodies used for immunofluorescence (IF) were Alexa Fluor 647-conjugated donkey anti-goat (catalog #A11057) and Alexa Fluor 568-conjugated donkey anti-rabbit (catalog #A21206) or Alexa Fluor 488-conjugated donkey anti-rat (catalog #A21208), all in 1:200 dilution (Life Technologies, Guilford, CT, USA). Sections were mounted under coverslips using Vectashield fluorescent mounting media with 46-diamidino-2-phenylindole (DAPI; catalog #H-1200; Vector Laboratories.) All the visualizations of the slides were done with a laser scanning confocal microscope (LSM 710; Zeiss) and the ZEN software (Carl Zeiss).

The immunoreactivity of Abs was semi-quantitatively evaluated using the H-score. The score value was derived by summing the percentage of cells that stained at each intensity category and multiplying that value by the weighted intensity of the staining [28]. For quantification of CD31 (a specific marker for vessels), we used the microvessel density (MVD) method [29]. The area with the greatest density of CD31 positive endothelial cells was designated as a spot, and then stained lesions were counted on at least five separate spots in high-power fields ($\times 400$). All stained endothelial cells or cell clusters were counted as one microvessel, and the MVD was defined as the sum of vessels found at all spot lesions.

Statistical analysis

Independent t-test or one-way analysis of variance with the post-hoc Dunnett or Tukey was used as appropriate to assess the difference in continuous variables among the groups. These data are presented as the mean \pm standard error of the mean (SEM). Statistical computation was performed using the Statistical Package for Social Science, version 12.0 software (SPSS, Chicago, IL), and P -value < 0.05 were considered statistically significant.

Results

Treatment restores endometrial histology

In pilot experiments to assess whether thinning of the EM is effectively induced by ethanol, we instilled either 95% ethanol or PBS (50 μL) into the uterine cavity. After 2 weeks, the endometrial epithelium was confirmed to have thinned EM with reduced number of glands in the stroma of the uterus in mice that received 95% ethanol

(Figure 1B, right). In contrast, the uterine structure was intact in mice that received PBS (Figure 1B, left).

The histologic images for the uterine horns from all groups are shown in Figure 2A and B (hematoxylin and eosinophil (H&E) staining). The endometrial epithelium was thick and extensively branched in the CXCL12, BMDCs, and the CXCL12 + BMDC treatment groups, whereas it was thin and dilated in PBS-treated mice.

To further evaluate the regeneration of the uterine structures, we assessed histologic parameters including the number of glands, mean values of total section area, stroma area, and luminal epithelial area (LEA) measured from each section by optical microscopy (eclipse 80i instrument; Nikon, Tokyo, Japan). The three treatment groups displayed significantly larger LEA, stroma area, and increased glandular numbers in the stroma, compared to the PBS group (Table 1). When these parameters were compared to sham control mice with normal EM, no significant difference was found between each treatment group versus the sham mice.

Recruitment of BMDCs, cell proliferation, and vascularization

The number of GFP BMDCs recruited into different groups (PBS, BMDCs, and CXCL12 + BMDCs) was determined by counting the GFP-positive cells. As shown in Figure 3A, GFP cells were recruited into the uterus of groups treated with BMDCs (middle), and CXCL12 + BMDCs (right), while no GFP cells were identified in the PBS-treated group. The mice group that was treated with both CXCL12 and BMDCs together showed a trend towards a higher number of GFP cells (10.8 ± 2.8) than the BMDC group (5.3 ± 0.9); however, the difference was not statistically significant. Further, we also tracked the migration of bone marrow-derived immune and nonimmune cells into the thin EM. We detected nonimmune cells in thin EM of mice treated with BMDCs expressing GFP compared to thin EM of mice received PBS treatment. These nonimmune mesenchymal cells were GFP positive, CD45 negative, and F4/80 negative (Figure 3B). Endogenous immune cells were positive for CD45 and/or F4/80 (macrophages) and also negative for GFP as shown in Figure 3B. We also found the majority of bone marrow-derived immune cells in thin EM of mice treated with BMDCs that were GFP+; these cells were could be positive for CD45 but negative for F4/80. While CD45+ cells and F4/80 positive cells were also detected as shown in Supplemental Figure S1. Both nonimmune mesenchymal cells and immune cells contribute to the population of cells engrafting the uterus after BMDC treatment.

To assess cellular proliferation and vascularization, we performed immunohistochemistry (IHC) for Ki-67 and CD31, respectively, in uterine tissues. Ki-67 was present in the nuclei of endometrial epithelial cells and stromal cells in all the groups (Figure 4A). In endometrial epithelium, the Ki-67 immunoreactivity was significantly higher in the CXCL12 ($P = 0.001$), BMDC ($P = 0.012$), and co-treatment ($P < 0.001$) groups when compared to the PBS control group as shown in Figure 4C by H-score evaluation of immunostained sections. In addition, the Ki-67 staining in the stroma was increased in the CXCL12 group ($P = 0.003$) and the CXCL12 + BMDC group ($P = 0.003$) compared to the PBS group, but there was no significant difference between the BMDC and PBS treatment groups. IHC for CD31 revealed more vascularization in the stroma in all treatment groups (Figure 4B), and the MVD scores were significantly higher across all treatment groups compared to the PBS group (Figure 4D).

Differential expression of cytokines and biochemical markers of uterine receptivity

We evaluated the expression of several cytokines and adhesion molecules that have been described to be involved in implantation. LIF mRNA levels were significantly upregulated in the CXCL12 ($P = 0.028$), BMDC ($P = 0.049$), and CXCL12 + BMDC ($P = 0.003$) groups compared with the PBS-treated group (Figure 5A). IHC showed that LIF was localized in the cytoplasm of the luminal and glandular epithelia (Figure 5B), and its immunoreactivity was statistically higher in all three treatment groups compared to the PBS group as determined by evaluation of percent of staining area (Figure 5C).

The qRT-PCR results for pro- and anti-inflammatory cytokines, integrins (ITGs), and MMPs are shown in Figure 6. The mRNA expression of the IL-1 β proinflammatory cytokine was significantly decreased in mice treated with CXCL12 ($P = 0.029$), BMDCs ($P = 0.021$), or both ($P = 0.032$). However, IL-6 mRNA was upregulated only in the co-treatment group ($P = 0.018$). ITG β 3 mRNA expression was significantly upregulated in all three treatment groups ($P < 0.05$) compared to the PBS-treated group while no significant changes observed for ITG α v. The mRNA levels of MMP-2 and MMP-9 were significantly downregulated ($P < 0.05$) by BMDCs or CXCL12 + BMDC treatments compared to PBS treatment, while CXCL12 treatment alone did not have an effect.

Bone marrow or CXCL12 treatment improved fertility

All of the five sham mice became pregnant (for sham mice—laparotomy and hemostatic clips were applied on the bilateral uterine horns for 5 min as performed in other experimental groups; however, no ethanol was instilled). None of the mice with ethanol-induced thin EM that were subsequently treated with control became pregnant during 60 days of mating. Two of the five mice in the CXCL12 and the BMDC-treated groups became pregnant, while three of the five mice in the co-treatment group conceived (Table 2). The time to pregnancy and mean pup weight did not differ among any of the groups. However, the mean litter size was lower in the CXCL12 or BMDC-treated group versus sham group ($P = 0.04$ and $P = 0.04$), respectively.

Discussion

The uterine EM is a dynamic tissue that undergoes cyclic proliferation, differentiation, tissue breakdown, and regeneration during reproductive periods. The main objective of these physiological processes is the successful implantation of the embryo and maintenance of the resulting pregnancy [30]. Accordingly, a persistent thin EM during the menstrual cycle in women who are planning a pregnancy or in ART cycles is not desirable and can result in a lower implantation rate or recurrent implantation failure (RIF).

In this study, we demonstrate that administration of CXCL12 or BMDCs significantly improved the endometrial growth/expansion in mice with thin EM, and increased the amount of stroma and number of glands. The underlying pathogenesis of persistent thin EM remains to be defined; however, angiogenesis is thought to be fundamental in supporting endometrial growth, which provides vascularized receptivity during implantation [31, 32]. The observed increased immunoreactivity of CD31 and Ki-67 in mice treated with CXCL12 or BMDCs indicates that both molecules contribute to restoration of the uterine structures by promoting vascularization and cellular proliferation in mice with thin EM. Transplantation of BMDCs

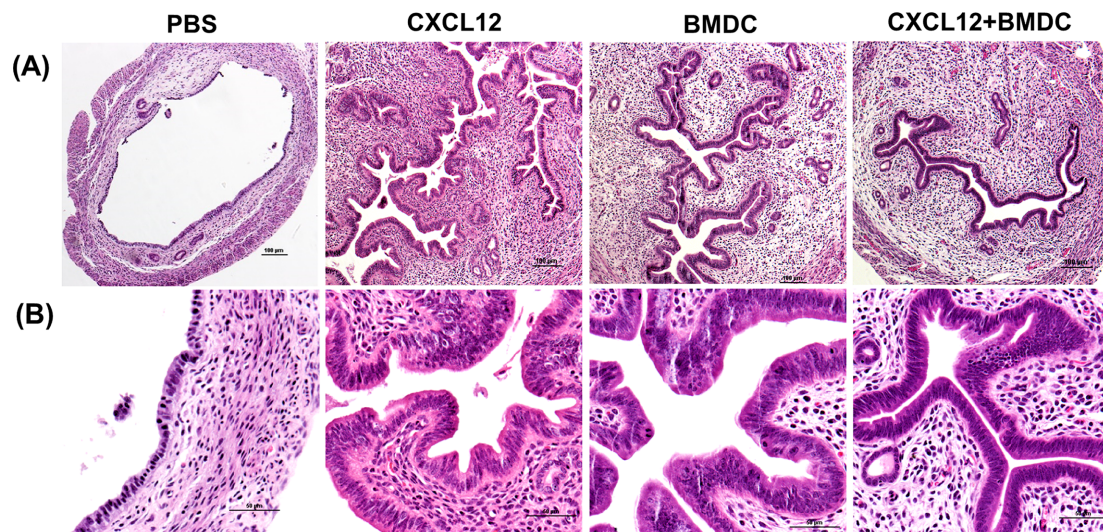


Figure 2. CXCL12/BMDCs treatments stimulate endometrial cell proliferation. (A and B) Representative micrographs of H&E staining showing increased thickness of endometrial epithelium after treatment with CXCL12, BMDCs, or both, compared to PBS treatment. (A: $\times 100$ and B: $\times 400$).

Table 1. Comparison of histological parameters.

	Sham (no ethanol)	Groups				P-value
		PBS	CXCL12	BMDCs	CXCL12 + BMDCs	
Glands #	40.5 \pm 5.8	8.4 \pm 2.5	31.6 \pm 4.5**	24.8 \pm 6.0*	36.0 \pm 6.6**	0.005
Diameter (mm)	1.83 \pm 0.09	1.05 \pm 0.06	1.64 \pm 0.10**	1.45 \pm 0.13*	1.45 \pm 0.07*	0.002
Total area (mm ²)	2.45 \pm 0.22	0.83 \pm 0.09	2.05 \pm 0.28**	1.82 \pm 0.33*	1.96 \pm 0.28*	0.010
Stroma (mm ²)	1.09 \pm 0.15	0.30 \pm 0.05	0.94 \pm 0.12**	0.81 \pm 0.09*	1.08 \pm 0.12**	<0.001
LEA (mm ²)	0.191 \pm 0.022	0.027 \pm 0.005	0.177 \pm 0.037**	0.182 \pm 0.037**	0.191 \pm 0.016**	0.001

LEA: luminal epithelial area, data are expressed as the mean \pm SEM.

* $P < 0.05$.

** $P < 0.01$; each group vs. PBS group by post-hoc Dunnett test.

has been shown to be beneficial in endometrial regeneration in previous rodent models of thin EM [23, 24]. Our findings agree with the prior findings; the expression of LIF and ITG was upregulated, while proinflammatory cytokine, such as IL- β , was decreased in mice treated with BMDCs. With regard to the biological functions of stem cells in the repair of damaged tissue, several mechanisms mediated by stem cells have been suggested, including activation of endogenous stem/progenitor cells, release of trophic factors that enhance neovascularization, and modulation of immune responses [33, 34].

A novel finding in the present study is that administration of CXCL12 also improved endometrial regeneration in mice with thin EM; effects of CXCL12 were comparable with those of BMDCs in analyses of histologic and biochemical markers. CXCL12 is recognized as the most potent chemoattractant of BMDCs and also displays a broad range of immunomodulatory actions and stimulatory effects for angiogenesis [35, 36]. The endogenous expression of CXCL12 is increased in response to various injuries and recruits mesenchymal stem cells to the damaged sites enabling tissue repair [37–40]. With the increased understanding of stem cell biology, recent studies have focused on the potential therapeutic capacities of this chemokine in a variety of conditions using experimental models of locally induced inflammation, nerve damage, or traumatic wounds [16, 41, 42]. We previously described a murine Asherman syndrome model where CXCL12 augmentation after uterine injury markedly reduced the formation of endometrial fibrosis, suggesting a role for

CXCL12 in preventing progressive uterine fibrosis and adhesions [13].

Another interesting finding in this study is that the expressions of MMP-2 and MMP-9 were significantly regulated by treatment with BMDCs. MMPs are a family of zinc-dependent proteolytic enzymes capable of degrading and rebuilding the extracellular matrix, and also play a role in cell migration [43]. Studies in humans show that MMP-2 and MMP-9 are present in endometrial stromal cells and may have an integral role in embryo implantation [44, 45]. Although the biological implication of MMPs in persistently thin EM is unclear, a prior study reported that overexpression or hyperactivity of MMP-2 or -9 in the uterine cavity is negatively associated with successful implantation in women with RIF [46]. The authors suggested that increased expression of MMPs or activity in uterine cavity is due to chronic and/or mild inflammation in the EM and likely reflects an unfavorable environment in the endometrial cavity for the implantation process. Women with RIF who were treated with antibiotics and a corticosteroid displayed reduced MMP activity in the uterine cavity, suggesting the improvement of the uterine environment [44]. Therefore, the finding of decreased MMP levels after treatment with BMDC and CXCL12 + BMDCs in our study may be explained by the development of intrauterine inflammation in thin EM, with the subsequent amelioration of the inflammation by BMDCs. Administration of CXCL12 alone did not demonstrate a regulatory effect on MMPs. A prior study identified the expression

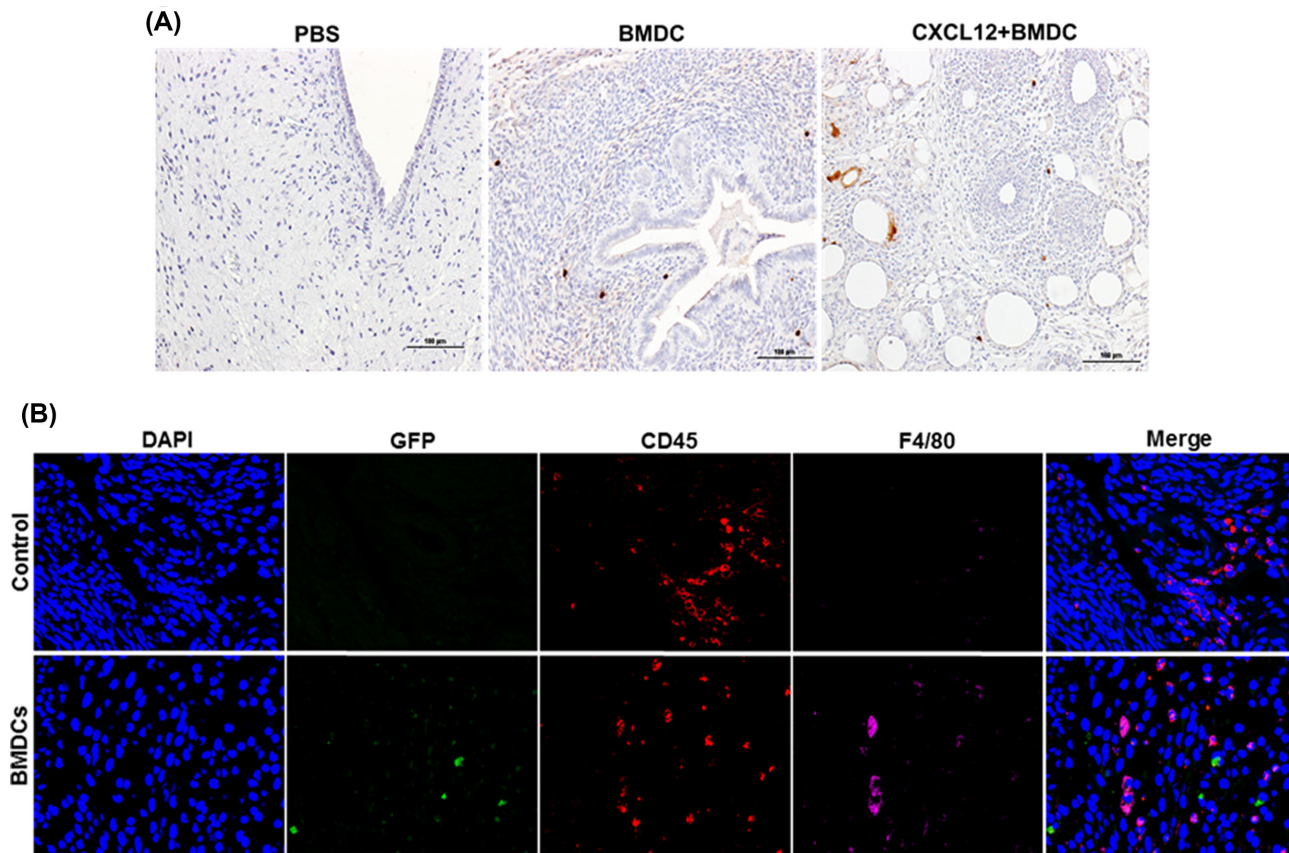


Figure 3. Recruitment of BMDCs. (A) Immunohistostaining of GFP with anti-GFP antibody showing the number of GFP⁺ cells recruited into different treatment groups: PBS (left), BMDC (middle), and CXCL12 + BMDC (right) ($\times 200$). (B) Representative images of IF of thin EM sections from mice treated with PBS (control) or BMDCs. Sections were co-stained with anti-GFP antibody (green), anti-CD45 (red), and anti-F4/80 antibody (magenta) to demonstrate the engraftment of immune and nonimmune cells into the uterus. Nuclei were stained by DAPI and are shown in blue. No GFP + BMDCs are noted in the controls, as expected. GFP + nonimmune cells (mesenchymal cells) are present in the EM of mice treated with BMDCs; these cells are both CD45 and F4/80 negative. Scale bar: 40 μm .

patterns of CXCL12 in normal human endometrial cells, where *in vitro* CXCL12 treatment had no significant effects on MMP production from the endometrial and epithelial cells [47]. It is likely that the CXCL12 effect is due to BMDC recruitment rather than a direct effect of CXCL12 on thin EM.

The pregnancy outcomes revealed relatively higher pregnancy rates in mice treated with CXCL12 (2/5), BMDCs (2/5), and CXCL12 + BMDCs (3/5) compared to PBS-treated mice (0/5). Although the pregnancy rates in these groups were not as high as the sham mice (5/5), these data suggest that both CXCL12 and BMDCs increase the success of implantation by facilitating functional and structural regeneration.

It still remains to be defined whether the concurrent administration of CXCL12 and BMDCs has a greater effect on endometrial regeneration than either molecule used alone. We were not able to observe a difference in histologic and chemical markers among the three treatment groups, with the exception that IL-6 was significantly upregulated and trended toward better pregnancy outcomes in the combined treatment group. Several reasons can be offered. As we described previously, BM-derived mesenchymal stem cells are recruited to the EM in response to any injury [15]. In the present study, ethanol-induced injury could recruit both endogenous BMDSCs of the host and/or administered BMDSCs from GFP mice to the uterus. The presence of both immune and non-immune cells in the thin EM of mice revealed that both types of

cells might have contributed to the regeneration of normal EM from thin EM. Some of the nonimmune cells detected in the thin EM of mice treated with BMDCs likely have role in the regeneration of EM. These nonimmune cells may be BMDCs stem cells but further characterization is needed to confirm them as stem cells. However, we could not track the engraftment of endogenous BMDSCs that were potentially mediated by CXCL12. Another possible explanation is that administration of CXCL12 has a therapeutic effect on endometrial regeneration by enhancing trophic effects, such as immunomodulation or stimulation of angiogenic factors, in addition to its recruitment of stem cells. Activation of immune response to injury is critical for tissue repair and regeneration, and accumulating evidence supports the comprehensive roles of CXCL12 for various immune components including macrophages, monocytes, and chemo/cytokines [18, 20, 48–50].

Conclusion

In summary, we demonstrate a beneficial effect of CXCL12 as well as BMDCs on the thin EM in a murine model, where they promote the restoration of endometrial proliferation, modulate biochemical markers related to endometrial receptivity, and improve the success of conception. Further studies regarding the CXCL12-mediated molecular mechanisms involved in regeneration of endometrial growth/physiology will help to better understand the

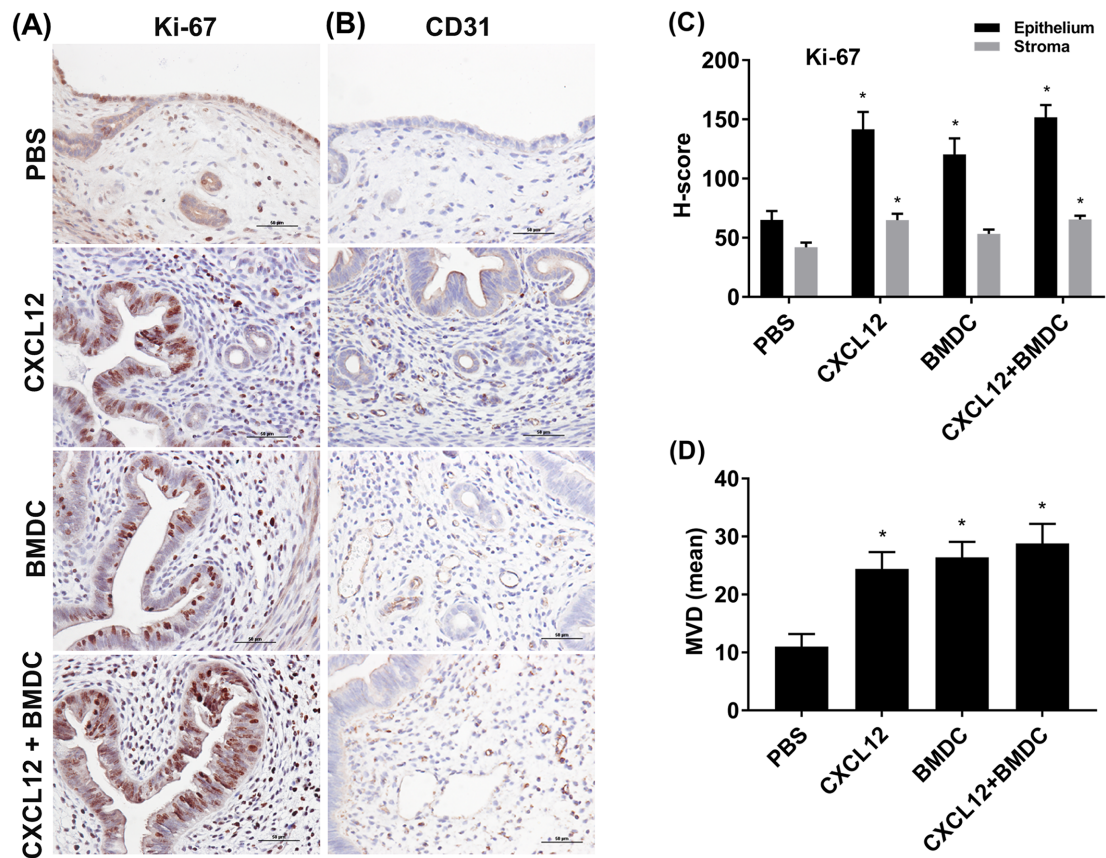


Figure 4. Immunostaining analysis of Ki-67 and CD31. Sections from uterine tissues of all treatment groups were stained with anti-Ki-67 (A) and anti-CD31 (B) antibodies ($\times 400$). (C) H-score showing the intensity of Ki-67 staining in epithelium and stroma for each treatment. (D) Showing MVD by CD31 staining. Data are expressed as the mean \pm SEM. * $P < 0.05$ vs. PBS group; ** $P < 0.01$ vs. PBS group.

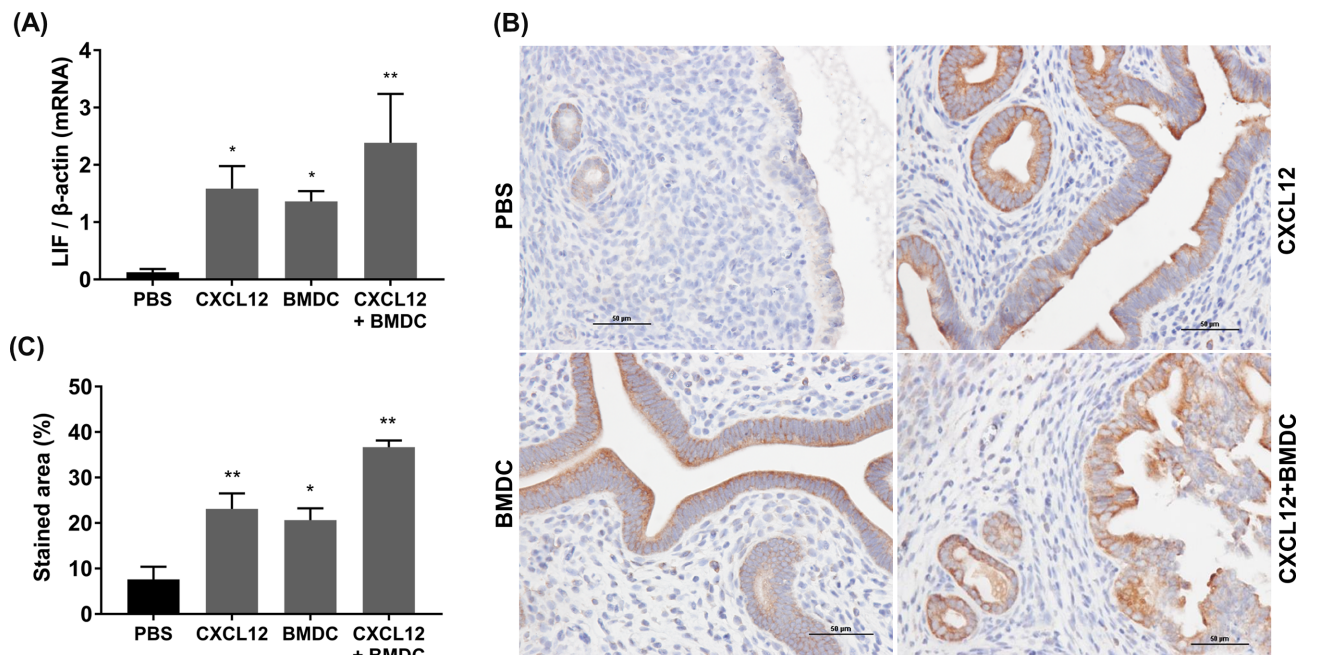


Figure 5. LIF mRNA and protein expression. (A) mRNA levels by qRT-PCR. (B) Immunostaining for anti-LIF ($\times 400$). (C) Quantitative analysis for immunostaining area (%). Data are expressed as the mean (%) \pm SEM. * $P < 0.05$ vs. PBS group; ** $P < 0.01$ vs. PBS group.

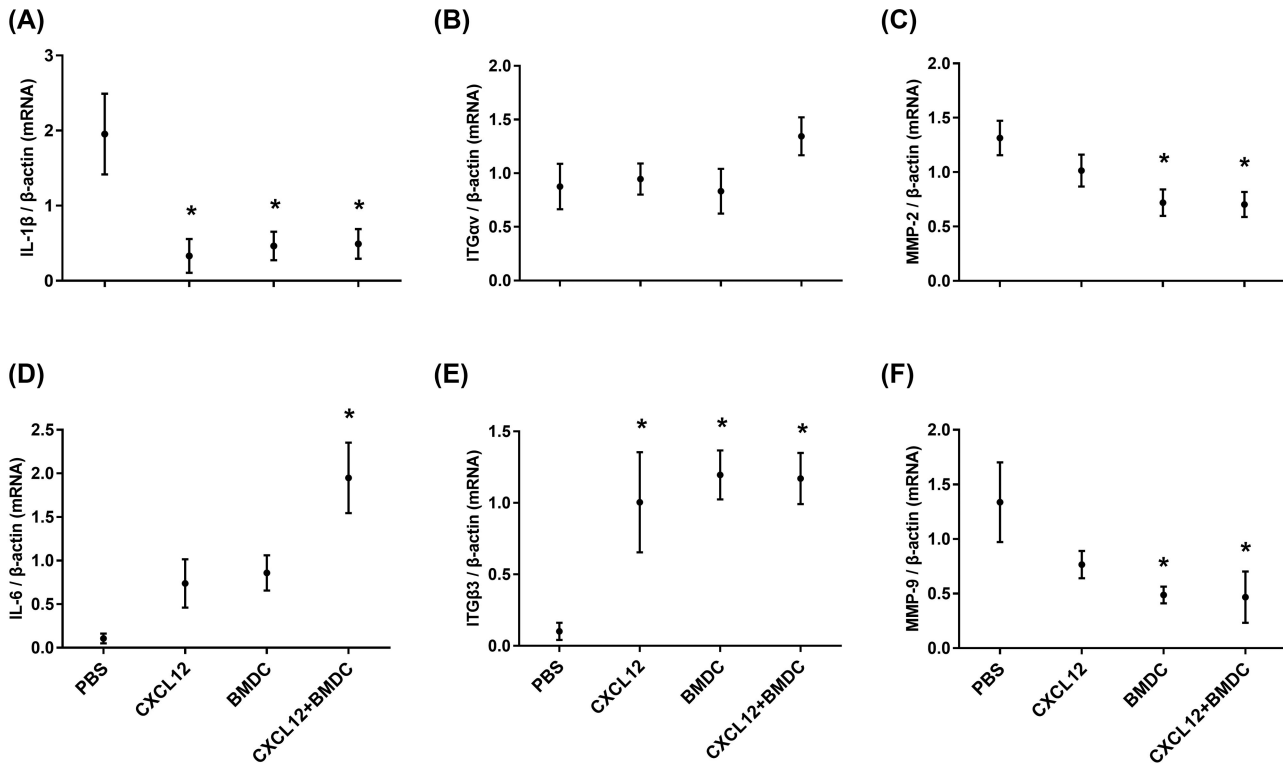


Figure 6. mRNA expression levels of uterine receptivity markers by qRT-PCR. Interleukins: IL-1 β (A) and IL-6 (B); ITGs: ITG α v (C) and ITG β 3 (D); and MMPs: MMP-2 (E) and MMP-9 (F). Data are expressed as the mean \pm SEM. * denotes statistical significance ($P < 0.05$) compared to PBS treatment group. Data represent three individual experiments and each experiment was carried out in duplicate.

Table 2. Pregnancy outcomes for the experimental treatment groups and sham control.

	Sham	Thin EM treatment groups				P-value
		PBS	CXCL12	BMDCs	CXCL12 + BMDCs	
Pregnancy case/total	5/5	0/5**	2/5	2/5	3/5***	0.04
Time to pregnancy, day [†]	10.0 (1–18)	–	21.5 (18–23)	11.0 (6–16)	10.0 (6–14)	NS
Litter size	7.8 \pm 1.5	–	3.5 \pm 0.5*	3.5 \pm 0.5*	5.0 \pm 1.5	0.015
Pup weight (g, mean)	1.36 \pm 0.01	–	1.40 \pm 0.04	1.40 \pm 0.03	1.42 \pm 0.04	NS

NS: not significant

* $P < 0.05$; each group vs. sham group by post-hoc Tukey test.

** $P = 0.001$ compared to sham control by Chi Square test with Yates correction.

*** $P = 0.04$ compared to PBS-treated control.

[†]Data expressed as the median with range.

roles of CXCL12, and will help determine its value as a therapeutic target.

Supplementary data

Supplementary data are available at [BIOLRE](https://doi.org/10.1080/00016344.2019.1634444) online.

Supplementary Figure S1. Analysis of immune cells after BMDCs engraftment by Fluorescence confocal microscopy. Representative IF images of thin endometrial tissue sections from mice treated with PBS (control) or BMDCs. Sections were co-stained with anti-GFP antibody (green), anti-CD45 (red), and anti-F4/80 antibody (magenta). Nuclei were stained by DAPI and are shown in blue. White arrows show the presence of GFP cells expressing CD45 (leukocytes), while yellow arrows show the presence of macrophages derived from BMDC treatment. Scale bar: 40 μ m.

Acknowledgments

We thank Shafiq Shaikh for providing GFP mice and assistance in extracting bone marrow-derived cells from GFP mice, Aya Tal and Sepide Nematian for their suggestions and technical support.

References

- Isaacs JD, Jr, Wells CS, Williams DB, Odem RR, Gast MJ, Strickler RC. Endometrial thickness is a valid monitoring parameter in cycles of ovulation induction with menotropins alone. *Fertil Steril* 1996; 65:262–266.
- Weissman A, Gotlieb L, Casper RF. The detrimental effect of increased endometrial thickness on implantation and pregnancy rates and outcome in an in vitro fertilization program?. *Fertil Steril* 1999; 71:147–149.
- Kasius A, Smit JG, Torrance HL, Eijkemans MJ, Mol BW, Opmeer BC, Broekmans FJ. Endometrial thickness and pregnancy rates after IVF: a

- systematic review and meta-analysis. *Hum Reprod Update* 2014; 20:530–541.
4. Gonen Y, Casper RF, Jacobson W, Blankier J. Endometrial thickness and growth during ovarian stimulation: a possible predictor of implantation in in vitro fertilization. *Fertil Steril* 1989; 52:446–450.
 5. Abdalla HI, Brooks AA, Johnson MR, Kirkland A, Thomas A, Studd JW. Endometrial thickness: a predictor of implantation in ovum recipients? *Hum Reprod* 1994; 9:363–365.
 6. Richter KS, Bugge KR, Bromer JG, Levy MJ. Relationship between endometrial thickness and embryo implantation, based on 1,294 cycles of in vitro fertilization with transfer of two blastocyst-stage embryos. *Fertil Steril* 2007; 87:53–59.
 7. Urman B, Mercan R, Alatas C, Balaban B, Isiklar A, Nuhoglu A. Low-dose aspirin does not increase implantation rates in patients undergoing intracytoplasmic sperm injection: a prospective randomized study. *J Assist Reprod Genet* 2000; 17:586–590.
 8. Frattarelli JL, Miller BT, Scott RT, Jr. Adjuvant therapy enhances endometrial receptivity in patients undergoing assisted reproduction. *Reprod Biomed Online* 2006; 12:722–729.
 9. Glujovsky D, Pesce R, Fiszбайн G, Sueldo C, Hart RJ, Ciapponi A. Endometrial preparation for women undergoing embryo transfer with frozen embryos or embryos derived from donor oocytes. *Cochrane Database Syst Rev* 2010; 9: Cd006359:1–53.
 10. Gleicher N, Kim A, Michaeli T, Lee HJ, Shohat-Tal A, Lazzaroni E, Barad DH. A pilot cohort study of granulocyte colony-stimulating factor in the treatment of unresponsive thin endometrium resistant to standard therapies. *Hum Reprod* 2013; 28:172–177.
 11. Du H, Taylor HS. Contribution of bone Marrow-Derived stem cells to endometrium and endometriosis. *Stem Cells* 2007; 25:2082–2086.
 12. Taylor HS. Endometrial cells derived from donor stem cells in bone marrow transplant recipients. *JAMA* 2004; 292:81–85.
 13. Sahin Ersoy G, Zolbin MM, Cosar E, Moridi I, Mamillapalli R, Taylor HS. CXCL12 promotes stem cell recruitment and uterine repair after injury in Asherman's Syndrome. *Mol Ther Methods Clin Dev* 2017; 4:169–177.
 14. Alawadhi F, Du H, Cakmak H, Taylor HS. Bone marrow-derived stem cell (BMDSC) transplantation improves fertility in a murine model of Asherman's syndrome. *PLoS One* 2014; 9:e96662.
 15. Du H, Naqvi H, Taylor HS. Ischemia/reperfusion injury promotes and granulocyte-colony stimulating factor inhibits migration of bone marrow-derived stem cells to endometrium. *Stem Cells Dev* 2012; 21:3324–3331.
 16. Villalvilla A, Gomez R, Roman-Blas JA, Largo R, Herrero-Beaumont G. SDF-1 signaling: a promising target in rheumatic diseases. *Expert Opin Ther Targets* 2014; 18:1077–1087.
 17. Kortessidis A, Zannettino A, Isenmann S, Shi S, Lapidot T, Gronthos S. Stromal-derived factor-1 promotes the growth, survival, and development of human bone marrow stromal stem cells. *Blood* 2005; 105:3793–3801.
 18. Bleul CC, Fuhlbrigge RC, Casanovas JM, Aiuti A, Springer TA. A highly efficacious lymphocyte chemoattractant, stromal cell-derived factor 1 (SDF-1). *J Exp Med* 1996; 184:1101–1109.
 19. Hattori K, Heissig B, Tashiro K, Honjo T, Tateno M, Shieh JH, Hackett NR, Quidoriano MS, Crystal RG, Rafii S, Moore MA. Plasma elevation of stromal cell-derived factor-1 induces mobilization of mature and immature hematopoietic progenitor and stem cells. *Blood* 2001; 97:3354–3360.
 20. Cheng JW, Sadeghi Z, Levine AD, Penn MS, von Recum HA, Caplan AI, Hijaz A. The role of CXCL12 and CCL7 chemokines in immune regulation, embryonic development, and tissue regeneration. *Cytokine* 2014; 69:277–283.
 21. Kim CH, Broxmeyer HE. In vitro behavior of hematopoietic progenitor cells under the influence of chemoattractants: stromal cell-derived factor-1, steel factor, and the bone marrow environment. *Blood* 1998; 91:100–110.
 22. Wang X, Mamillapalli R, Mutlu L, Du H, Taylor HS. Chemoattraction of bone marrow-derived stem cells towards human endometrial stromal cells is mediated by estradiol regulated CXCL12 and CXCR4 expression. *Stem Cell Res* 2015; 15:14–22.
 23. Jing Z, Qiong Z, Yonggang W, Yanping L. Rat bone marrow mesenchymal stem cells improve regeneration of thin endometrium in rat. *Fertil Steril* 2014; 101:587–594.e3.
 24. Zhao J, Zhang Q, Wang Y, Li Y. Uterine infusion with bone marrow mesenchymal stem cells improves endometrium thickness in a rat model of thin endometrium. *Reprod Sci* 2015; 22:181–188.
 25. Jing Z, Hong G, Yanping L. Development of an animal model for thin endometrium using 95% ethanol. *J Fertil In vitro* 2012; 2:1–4.
 26. Barr A, Manning D. *G Proteins Techniques of Analysis*. Boca Raton, FL: CRC Press, Inc; 1999:227–245.
 27. Livak KJ, Schmittgen TD. Analysis of relative gene expression data using real-time quantitative PCR and the 2⁻ΔΔCT method. *Methods* 2001; 25:402–408.
 28. Kim SH, Lee HW, Kim YH, Koo YH, Chae HD, Kim CH, Lee PR, Kang BM. Down-regulation of p21-activated kinase 1 by progestin and its increased expression in the eutopic endometrium of women with endometriosis. *Hum Reprod* 2009; 24:1133–1141.
 29. Weidner N. Current pathologic methods for measuring intratumoral microvessel density within breast carcinoma and other solid tumors. *Breast Cancer Res Tr* 1995; 36:169–180.
 30. Valdes CT, Schutt A, Simon C. Implantation failure of endometrial origin: it is not pathology, but our failure to synchronize the developing embryo with a receptive endometrium. *Fertil Steril* 2017; 108:15–18.
 31. Torry DS, Leavenworth J, Chang M, Maheshwari V, Groesch K, Ball ER, Torry RJ. Angiogenesis in implantation. *J Assist Reprod Genet* 2007; 24:303–315.
 32. Smith SK. Angiogenesis and implantation. *Hum Reprod* 2000; 15:59–66.
 33. Nagaya N, Kangawa K, Itoh T, Iwase T, Murakami S, Miyahara Y, Fujii T, Uematsu M, Ohgushi H, Yamagishi M, Tokudome T, Mori H et al. Transplantation of mesenchymal stem cells improves cardiac function in a rat model of dilated cardiomyopathy. *Circulation* 2005; 112:1128–1135.
 34. Zhang N, Li J, Luo R, Jiang J, Wang JA. Bone marrow mesenchymal stem cells induce angiogenesis and attenuate the remodeling of diabetic cardiomyopathy. *Exp Clin Endocrinol Diabetes* 2008; 116:104–111.
 35. Nagasawa T, Hirota S, Tachibana K, Takakura N, Nishikawa S, Kitamura Y, Yoshida N, Kikutani H, Kishimoto T. Defects of B-cell lymphopoiesis and bone-marrow myelopoiesis in mice lacking the CXC chemokine PBSF/SDF-1. *Nature* 1996; 382:635–638.
 36. Aiuti A, Webb IJ, Bleul C, Springer T, Gutierrez-Ramos JC. The chemokine SDF-1 is a chemoattractant for human CD34⁺ hematopoietic progenitor cells and provides a new mechanism to explain the mobilization of CD34⁺ progenitors to peripheral blood. *J Exp Med* 1997; 185:111–120.
 37. Abbott JD, Huang Y, Liu D, Hickey R, Krause DS, Giordano FJ. Stromal Cell-Derived Factor-1α Plays a critical role in stem cell recruitment to the heart after myocardial infarction but is not sufficient to induce homing in the absence of injury. *Circulation* 2004; 110:3300–3305.
 38. Askari AT, Unzek S, Popovic ZB, Goldman CK, Forudi F, Kiedrowski M, Rovner A, Ellis SG, Thomas JD, DiCorleto PE, Topol EJ, Penn MS. Effect of stromal-cell-derived factor 1 on stem-cell homing and tissue regeneration in ischaemic cardiomyopathy. *Lancet North Am Ed* 2003; 362:697–703.
 39. Hill WD, Hess DC, Martin-Studdard A, Carothers JJ, Zheng J, Hale D, Maeda M, Fagan SC, Carroll JE, Conway SJ. SDF-1 (CXCL12) is upregulated in the ischemic penumbra following stroke: association with bone marrow cell homing to injury. *J Neuropathol Exp Neurol* 2004; 63:84–96.
 40. Unzek S, Zhang M, Mal N, Mills WR, Laurita KR, Penn MS. SDF-1 recruits cardiac stem cell-like cells that depolarize in vivo. *Cell Transplant* 2007; 16:879–886.
 41. Wu Q, Ji FK, Wang JH, Nan H, Liu DL. Stromal cell-derived factor 1 promoted migration of adipose-derived stem cells to the wounded area in traumatic rats. *Biochem Biophys Res Commun* 2015; 467:140–145.
 42. Wang GD, Liu YX, Wang X, Zhang YL, Zhang YD, Xue F. The SDF-1/CXCR4 axis promotes recovery after spinal cord injury by mediating bone marrow-derived from mesenchymal stem cells. *Oncotarget* 2017; 8:11629–11640.
 43. Klein T, Bischoff R. Physiology and pathophysiology of matrix metalloproteases. *Amino Acids* 2011; 41:271–290.
 44. Yoshii N, Hamatani T, Inagaki N, Hosaka T, Inoue O, Yamada M, Machiya R, Yoshimura Y, Odawara Y. Successful implantation after reducing matrix metalloproteinase activity in the uterine cavity. *Reprod Biol Endocrinol* 2013; 11:37.

45. Salamonsen LA, Butt AR, Hammond FR, Garcia S, Zhang J. Production of endometrial matrix metalloproteinases, but not their tissue inhibitors, is modulated by progesterone withdrawal in an in vitro model for menstruation. *J Clin Endocrinol Metab* 1997; **82**:1409–1415.
46. Inagaki N, Stern C, McBain J, Lopata A, Kornman L, Wilkinson D. Analysis of intra-uterine cytokine concentration and matrix-metalloproteinase activity in women with recurrent failed embryo transfer. *Hum Reprod* 2003; **18**:608–615.
47. Laird SM, Widdowson R, El-Sheikhi M, Hall AJ, Li TC. Expression of CXCL12 and CXCR4 in human endometrium; effects of CXCL12 on MMP production by human endometrial cells. *Hum Reprod* 2011; **26**:1144–1152.
48. Julier Z, Park AJ, Briquez PS, Martino MM. Promoting tissue regeneration by modulating the immune system. *Acta Biomater* 2017; **53**:13–28.
49. Wan X, Xia W, Gendoo Y, Chen W, Sun W, Sun D, Cao C. Upregulation of stromal cell-derived factor 1 (SDF-1) is associated with macrophage infiltration in renal ischemia-reperfusion injury. *PLoS One* 2014; **9**:e114564.
50. Suzuki Y, Rahman M, Mitsuya H. Diverse transcriptional response of CD4+ T cells to stromal cell-derived factor SDF-1: cell survival promotion and priming effects of SDF-1 on CD4+ T cells. *J Immunol* 2001; **167**:3064–3073.